

## **DESIGN OF THE HIGH EFFICIENCY CIRCULAR HORN FEED FOR HIGH-POWER MICROWAVE SYSTEM**

**H. Li, J.-Y. Li, H.-Y. Wang, T.-M. Li, and Y.-H. Zhou**

School of Physical Electronics  
University of Electronic Science and Technology of China  
Chengdu, Sichuan 610054, China

**Abstract**—Design aspects of high efficiency profiled circular horn feeds with smooth wall for the high-power microwave (HPM) system are presented in this paper. The modal content at the circular aperture of horn necessary to closely approximate a linear polarized Gaussian distribution is established. Slope discontinuities along the axis of the horn are then used to generate the necessary waveguide modes with the appropriate amplitudes and phases at the aperture. The performance of the horn is calculated using the mode matching technique. Significant improvement in the performance of radiation over a straight conical horn can be achieved on the premise of high power capacity. The excellent correspondence between the simulations by MMT codes and CSTMWS (CST microwave studio) supports this conclusion.

### **1. INTRODUCTION**

High-power microwave (HPM) source is commonly used to describe microwave device that is typically IREBs-driven (the intense, relativistic electron beams), using interaction structures such as cavities to cause beam bunching and the conversion of beam kinetic energy into radio frequency (RF) energy [1]. An impressive increase in the power and operating frequency of HPM sources has taken place in the last few decades. At present, the HPM sources can generate coherent electromagnetic radiation with gigawatt-level. The Relativistic Klystron Amplifier of the Naval Research Laboratory has generated a power of 15 GW at a frequency of 1.3 GHz in a single-shot,  $\sim 50$  ns pulse [2]. The maximum power obtained with a single-mode

---

Corresponding author: H. Li (holly@uestc.edu.cn).

relativistic BWO in the X band was 3 GW with  $\sim 100$  J energy in a single pulse [3]. The efficient radiation of the intense electromagnetic wave generated by HPM source is an indispensable premise of such a HPM application as the directed energy weapon (DEW), radar system [4, 5].

Horn antennas are the most common aperture antennas, enjoying a great popularity as main radiator or feed horns in reflector antennas. Generally speaking, the near symmetry radiation patterns, low cross-polarization, and low sidelobe level are required properties for the efficient horn antennas. Corrugated horns can provide good beam patterns over a large bandwidth, widely used from millimeter to submillimeter wavelengths [6]. However, for the HPM radiation system, there is an additional need to provide the high power capacity [7]. The intense electromagnetic wave easily causes the breakdown between the grooves of throat in corrugated horn. The design approach presented in this paper is different from the traditional methods of improving the aperture efficiency through the use of smooth metallic wall construction of the multimode horn. So the high power capacity in the horn can be effectively guaranteed. The efficiency of the horns can be improved by introducing the level of higher order modes at the horn aperture by means of circularly symmetric discontinuities along the axis. The success of this approach has been verified by the close agreement between the two simulation results by CSTMWS and MMT codes respectively of two high efficiency horns in S band.

The steps necessary for the successful design of a multimode circular horn with high power capacity are as follows.

- a) Determine the ideal modal content at the horn aperture;
- b) Synthesize a profiled horn to give the desired radiation characteristics, such as aperture efficiency, return loss, and peak power density, by means of optimization of horn physical parameters. Performance simulations in synthesize process is carried out using the mode matching technique (MMT).

These steps are discussed below.

## 2. DETERMINATION OF MODAL CONTENT

In order to obtain the ideal radiation performances, the appropriate electric field distribution at horn aperture must be provided. The fundamental Gaussian beam (FGB) transversal electric field distribution can theoretically satisfy the requirements of symmetry radiation patterns, low cross-polarized, and low sidelobe level. Since the FGB mode is a solution of the paraxial wave equation in the free

space which can not meet the boundary condition of waveguide, mixing properly waveguide mode together to construct a FGB mode will be carried out [8].

The aperture distribution is assumed to be perfectly polarized in the  $\hat{y}$ -direction. Since closed form expressions for FGB transversal electric field distribution and waveguide modes at the aperture are given by [9]

$$\vec{E}_g(r, \varphi, \omega) = E_0 \cdot e^{-\left(\frac{r}{\omega}\right)^2} \cdot \left( \sin(\varphi) \cdot \vec{i}_r + \cos(\varphi) \cdot \vec{i}_\varphi \right) \quad (1)$$

$$\begin{aligned} \vec{E}_{mn}^e &= -\frac{J'_m\left(\frac{v_k r}{a}\right)}{a J_{m+1}(v_k)} \cos(m\varphi) \cdot \vec{i}_r \\ &\pm \frac{m}{v_k r} \frac{J_m\left(\frac{v_k r}{a}\right)}{J_{m+1}(v_k)} \sin(m\varphi) \cdot \vec{i}_\varphi \end{aligned} \quad (2)$$

$$\begin{aligned} \vec{E}_{mn}^h &= \pm \frac{m}{\sqrt{\mu_k^2 - m^2}} \frac{J_m\left(\frac{\mu_k r}{a}\right)}{r J_m(\mu_k)} \sin(m\varphi) \cdot \vec{i}_r \\ &- \frac{\mu_k}{\sqrt{\mu_k^2 - m^2}} \frac{J'_m\left(\frac{\mu_k r}{a}\right)}{a J_m(\mu_k)} \cos(m\varphi) \cdot \vec{i}_\varphi \end{aligned} \quad (3)$$

where  $\vec{E}_g$  is the linearly polarized fundamental Gaussian beam transversal electric field distribution, and  $\vec{E}_{mn}^e$  and  $\vec{E}_{mn}^h$  are the transversal electric field distributions of the TM and TE modes, respectively.  $\omega$  is the beam waist radius of FGB mode.  $J_m(x)$  is the Bessel function of the first kind of order  $m$  and argument  $x$ , and the prime associated with the Bessel function denotes the first derivative with respect to the argument.  $k = (m, n)$  is the mode index, and  $(r, \varphi)$  are the cylindrical coordinates.  $a$  is the guide radius;  $v_k/a$  and  $\mu_k/a$  are the cutoff wavenumber of TM mode and TE mode respectively. It is assumed that the horn is fed by a single-moded guide with the TE<sub>11</sub> mode. All the discontinuities are circularly symmetric. Consequently only the TE<sub>1n</sub> and TM<sub>1n</sub> modes can be excited. The required mode mixtures to synthesize the fundamental Gaussian beam mode with waveguide modes as Equation (4) can be obtained using a correlation integral between a guided mode and the fundamental Gaussian beam mode. These correlation integrals are defined as follows:

$$\vec{E}_g(r, \varphi, \omega) = \sum_n A_{1n}(\omega, \tau, \theta) \vec{E}_{1n}^e(r, \varphi) + \sum_n B_{1n}(\omega, \tau, \theta) \vec{E}_{1n}^h(r, \varphi) \quad (4)$$

$$A_{1n}(\omega) = \iint_{ap} E_g^* \cdot E_{1n}^e \cdot r dr d\varphi \quad (5)$$

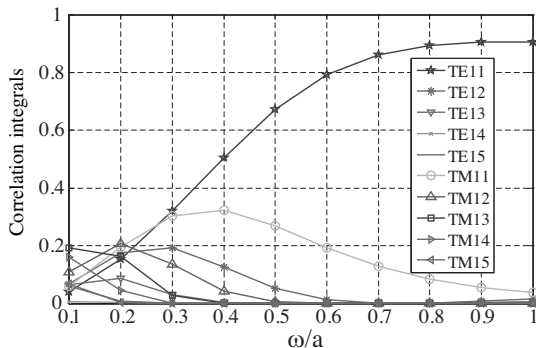


**Figure 1.** Mode content to construct a FGB transversal field distribution of beam waist  $\omega$  at aperture.

$$B_{1n}(\omega) = \iint_{ap} E_g^* \cdot E_{1n}^h \cdot r dr d\varphi \quad (6)$$

where  $\vec{E}_g^*(r, \varphi, \omega)$  is the conjugated expression of the FGB transversal electric field distribution. These correlation integrals  $A_{1n}$  and  $B_{1n}$  are the functions of the ratio between aperture radius  $a$  and beam waist  $\omega$ . The correlation integrals for the first five TE and TM modes have been evaluated and plotted in Fig. 1.

As shown in Fig. 1, when the ratio between  $\omega$  and radius is from 0.65 to 0.9, the mixture of TE and TM is the simplest mode mixture because it only involves two modes, and thus, it is relatively easy to generate [8]. It should be noted that, as approaches unity, the sidelobe-level of radiation pattern rise is inevitable, due to the truncation effect produced by the guide wall [see Figs. 2(a), (b), (c)]. The relative amplitude distributions of FGB transversal field with different beam waist  $\omega$  at aperture are plotted in Fig. 2(d).

The ratio of 0.65 is a very familiar point that widely used as HE<sub>11</sub> mode in the corrugated horn and the Potter horn [17]. Of course, in order to obtain the lower sidelobes, the smaller ratio should be accepted. The literature [8] proposed that adding some part of a Gaussian profiled horn antenna at its end can improve important far-field radiation pattern features of any existing conical horn, like sidelobe and cross-pol levels, while keeping its other far-field characteristics. In fact, the better features are achieved by changing the ratio using the additional part.

From the more general sense, the expansion method in this paper can be applied to the arbitrary field distribution at aperture. During the specific designation, we should choose appropriate modal content as our optimistic target according to the actual requirements

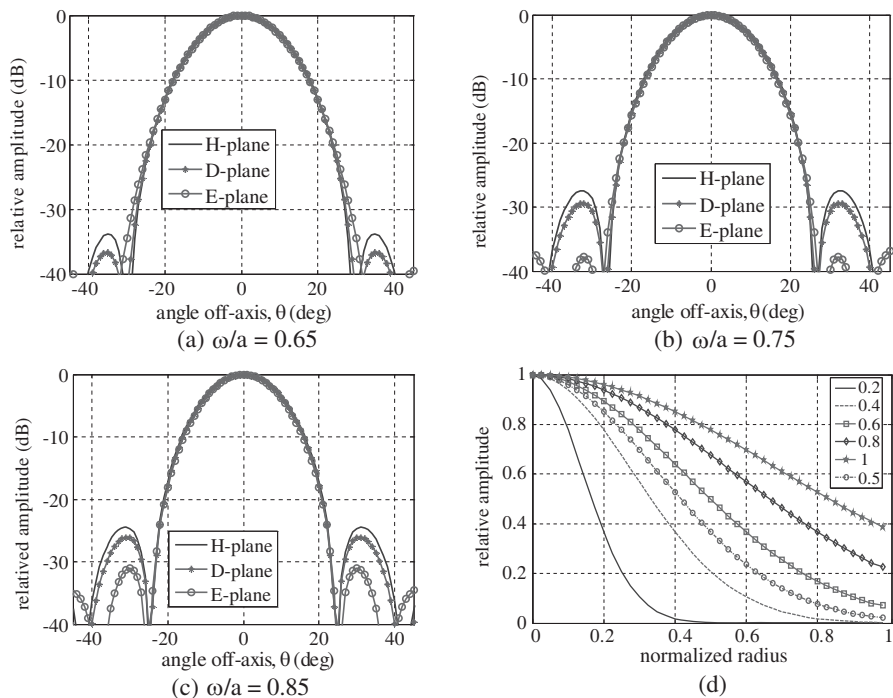


**Figure 2.** Radiation patterns and relative amplitude distributions of FGB transversal field of beam waist  $\omega$  at aperture.

in application. In this paper, in order to demonstrate the versatility of the synthesis method, we choose two different modal contents corresponding to the ratio of 0.65 and 0.5 respectively as the optimistic target.

### 3. SYNTHESIS OF PROFILED CIRCULAR HORNS

The method chosen here to excite the higher order modes employs slope discontinuity. This approach has higher power capacity and broader bandwidth performance than utilizing step discontinuity [10]. The structure of a profiled horn with multiple discontinuities is shown in Fig. 3.

In the usual application, since only one or two higher order TE and TM modes need to be generated and controlled in frequency bands, 3 or 4 slope discontinuities should suffice. But for the horn with oversized aperture, more slope discontinuities must be used since more modes need to be controlled. Since more parameters need to be optimized, a

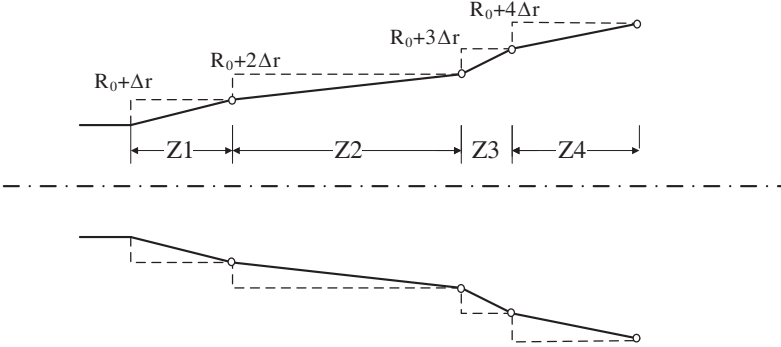


**Figure 3.** Multimode profiled horn and approximate model.

faster approach of synthesis is indispensable.

First of all, the specified horn profile is segmented into a series of slope circular waveguide sections with varying radii according to the number of sections. In order to speed up the calculation, the size of the varying radius ( $\Delta r$  in Fig. 3) of step is set equally. The design process only involves specifying the approximate axial locations ( $z_1, z_2$ , etc.) of the slope break points (see Fig. 3). The horn profile is linear in between these break points. In the proceeding of calculation by MMT [11, 12], each of the slope discontinuity is then segmented into a series of stepped circular waveguide sections with the same scale of varying radii that is less than  $0.02\lambda$  usually. Taking into account the radius of horn growing usually, the structure and generalized scattering matrices (GSM) of each step discontinuity are certain. So the next analyzing process includes three steps. Firstly calculate and save the GSM of all the stepped waveguide junctions which can be reused to improve speed of calculating performance of the tentative horn significantly. Then according to the axial distance of each step breakpoint, the phase shift matrices can be obtained. Finally, the horn performance is characterized by combining them to yield the overall scattering parameters.

The objective function is constituted by the error distance in the multi-dimension space of modal content and the input return loss which is given as

$$F = \sum_{k=1}^m \left( w_S S_k + w_A \sum_{i=1}^n (|A_{ki} - T|_i)^2 \right) \quad (7)$$

here,  $A$  and  $T$  represent the obtained model content by normality of phase and the desired value, respectively. The corresponding weights of functions are  $w_S$  and  $w_A$ .  $S$  indicates the return loss. The subscript

of  $k$  and  $i$  represent the index of frequency and model respectively. The number of frequency and model are  $m$  and  $n$ , respectively. Compared to the objective functions comprising the horn parameters [10, 15], like sidelobe and symmetry, the approach of using multi-dimension distance can significantly reduce the time consumed in the process of repeatedly calculating the radiation patterns. Table 1 demonstrates the consumed time of every procedure in the MMT analysis. In the optimization, a lots of horn models need to be analyzed. The novel method in the paper can avoid repeat calculations of radiation patterns and every S parameters matrix of step discontinuous.

**Table 1.** The consumed time of every procedure in the MMT analysis of the S band horn with 200 step discontinuous and 80 model.

S parameters matrix of step discontinuous	Combining the two successively S parameters matrixes	Radiation patterns
89.2s	0.44s	6.95s

Finding the optimum horn geometry that satisfies a pre-determined specification is done using a genetic algorithm (GA), which is a powerful computational method for solving optimization problems [13, 15, 16]. The GA differs substantially from more traditional search and optimization methods. They do not require derivative information or other auxiliary knowledge; only the objective function and corresponding fitness levels influence the directions of search. GA use probabilistic transition rules instead of deterministic ones. An important feature of the GA is that it avoids convergence to a local extremum by exploring the search space. Application of GA to horn design is made by associating the chromosome to each axial location ( $z$ ). The initial population of individuals (horns) is generated randomly. Through the processes of selection according to the objective function, crossover, mutation, the optimum can be achieved.

We have written mode matching technique and genetic algorithm codes and combined these into a horn design package with a graphical user interface. In the process of optimization, the simple binary GA has been used, which adopts the stochastic universal sampling routine, single-point crossover routine with probability of 0.9 and mutation probability of 0.7. The designations of high efficiency horn in S band have been carried out.

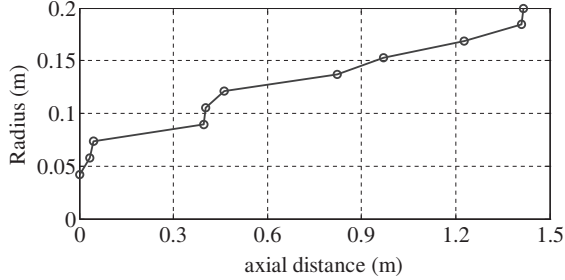


**Figure 4.** The profiled curve of horn #1.

#### 4. RESULTS

Firstly, a horn feed with symmetric mainlobe and sidelobes beneath  $-40$  dB in S band has been investigated. In order to satisfy the requirement of low sidelobes, the modal contents at aperture are chosen to correspond the FGB transversal field with the ratio of 0.5. The horn is composed of 10 slope discontinuities, an aperture diameter of 40 cm and an axial length of 141.54 cm shown in Fig. 4. The synthesis work was performed on the E5405 Intel Xeon CPU and takes 2.3 hours of computation, which can be substantially reduced by parallelization. The value of  $w_S$  and  $w_A$  used are 2 and 1 respectively. The normalized radiation patterns of the optimum horn and the ideal FGB transversal field are plotted in Fig. 5. The ideal and realized aperture modal contents are shown in Table 2. There are excellent correlations in the amplitude, phase and radiation patterns. The return loss is  $-32.7$  dB. The vector correlation coefficient of the field at aperture to an ideal FGB is 99.82% [14].

**Table 2.** Mode content of actual horn and ideal FGB transversal field.

Mode	Ideal		Actual		Mode	Ideal		Actual	
	Amplitude	Phase	Amplitude	Amplitude		Amplitude	Phase	Amplitude	Phase
TE <sub>11</sub>	1	0	1	0	TM <sub>11</sub>	0.6326	180	0.6536	176.47
TE <sub>12</sub>	0.2837	180	0.3171	179.63	TM <sub>12</sub>	0.0970	0	0.0827	22.02
TE <sub>13</sub>	0.0236	0	0.0078	-25.36	TM <sub>13</sub>	0.0122	180	0.0078	-74.23
TE <sub>14</sub>	0.0011	0	0.0046	-135.15	TM <sub>14</sub>	cutoff	-	-	-

Then, a horn of S band with symmetric mainlobe and sidelobes beneath  $-27$  dB in 14% frequency bandwidth from 2.6 GHz to 3.0 GHz for the frequency-agile Relativistic Magnetron has been investigated. For the optimization of this horn, the values of  $w_S$  and  $w_A$  used are

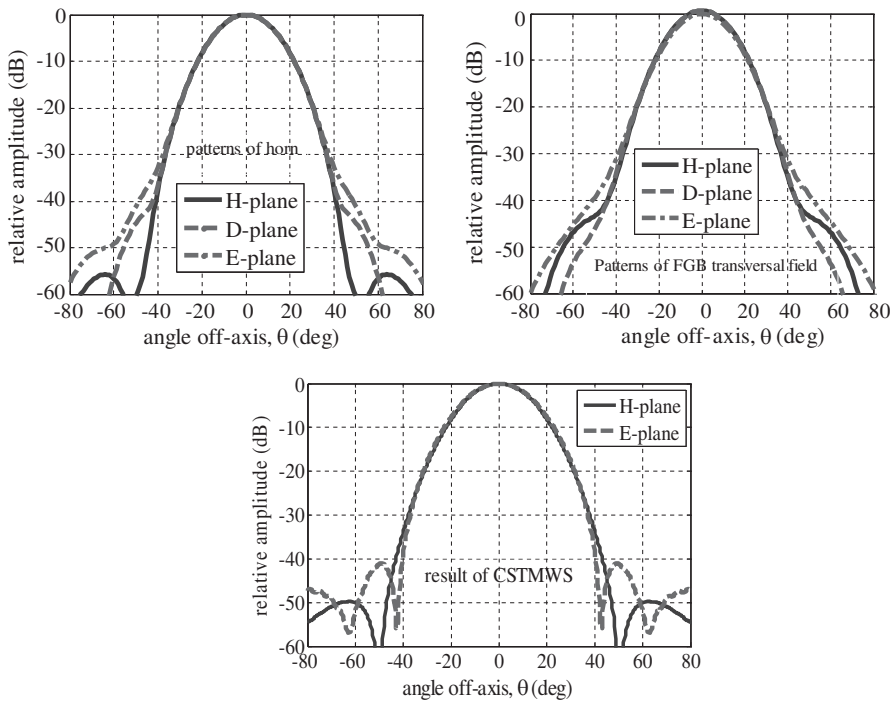


**Figure 5.** Comparisons between radiation patterns of horn #1 and FGB transversal field.

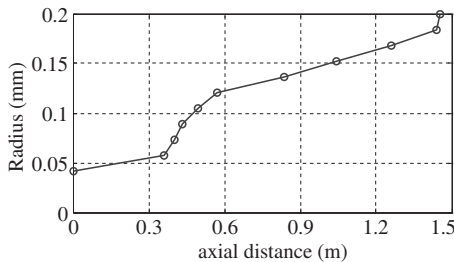


**Figure 6.** The profiled curve of horn #2.

1 and 1, respectively. The parameters of  $T$  are the values of the ideal aperture modal contents corresponding to ratio of 0.65. The horn has 10 slope discontinuities, an aperture diameter of 40 cm and an axial length of 145.32 cm shown in Fig. 6. The synthesis work was performed on the E5405 Intel Xeon CPU and almost takes 8 hours of computation. The maximum return loss is below  $-24$  dB in the frequency band. The normalized radiation patterns are plotted in Fig. 7 at the band edge

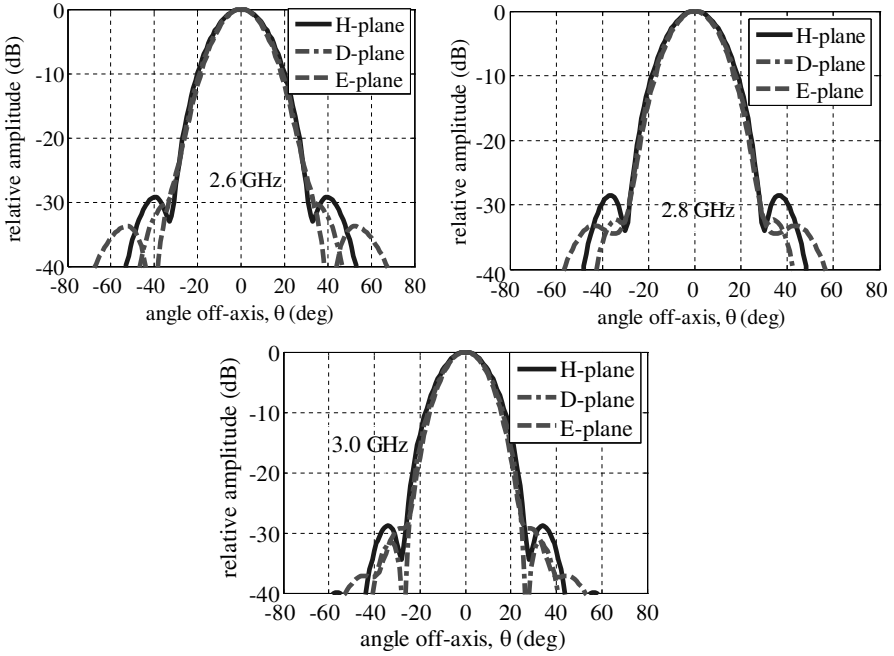


**Figure 7.** Far-field radiation patterns of the horn #2 with broad frequency band.

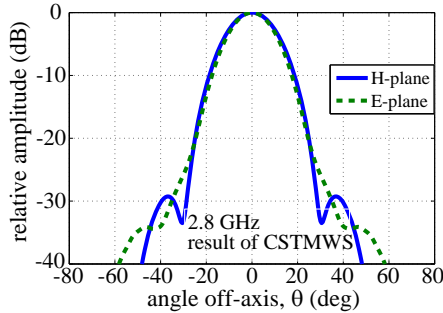


**Figure 8.** Far-field radiation patterns of the horn #2 simulated by CSTMWS at the centre frequency.

and center frequencies. The simulated radiation pattern by CSTMWS is plotted in Fig. 8. There is an excellent correlation in the mainlobe between the prediction and simulation. At the same time, the patterns of optimum horn close to the ones of ideal FGB transversal field in Fig. 2(a) demonstrate the validity of the synthesis approach.

## 5. CONCLUSION

This paper presents the design of a high-efficiency circular horn with smooth wall construction that is highly desirable for the HPM application. First of all, the FGB field distribution are analyzed in order to determine the ideal modal content at the horn aperture. Secondly, the objective function directly using the modal content are present, which can improve the speed of the synthesis in the GA optimizer. At the same time, the technique to reuse GSM of all the stepped waveguide junctions has been adopted which can further improve the velocity of optimizer. The broad bandwidth high efficiency horn for the frequency-agile Relativistic Magnetron and a horn feed with low sidelobes are designed. Design results agree well with the simulation by CSTMWS, which demonstrates the validity of the approach .

## REFERENCES

1. Barker, R. J. and E. Schamiloglu, *High-power Microwave Sources and Technologies*, Wiley-IEEE Press, Jun. 2001.
2. Friedman, M., R. Fernsler, S. Slinker, R. Hubbard, and M. Lampe, "Efficient conversion of the energy of intense relativistic electron beams into RF waves," *Phys. Rev. Lett.*, Vol. 75, 1214, 1995.
3. Gunin, A. V., "Relativistic X-band BWO with 3-GW output power," *IEEE Trans. Plasma Sci.*, Vol. 26, 326–331, Jun. 1998.
4. Radaky, W. A. and C. E. Baum, "Introduction to the special issue on high-power electromagnetics (HPEM) and intentional electromagnetic interference (IEMI)," *IEEE Transaction on Electromagnetic Compatibility*, Vol. 46, No. 3, 314–321, 2004.
5. Wang, H., J. Li, H. Li, K. Xiao, and H. Chen, "Experimental study and spice simulation of CMOS inverters latch-up effects due to high power microwave interference," *Progress In Electromagnetics Research*, PIER 87, 313–330, 2008.
6. Clarricoats, P. J. B. and A. D. Olver, *Corrugated Horns for Microwave Antennas*, IEE Press, 1984.
7. Agee, F. J., "Evolution of pulse shortening research in narrow band, high power microwave sources," *IEEE Trans. Plasma Sci.*, Vol. 26, 235, 1998.
8. Gonzalo, R. and J. Teniente, "Improved radiation pattern performance of Gaussian profiled horn antennas," *IEEE Transactions on Antennas and Propagation*, Vol. 50, 1505–1513, Nov. 2002.
9. Huang, H. J., *Microwave Theory*, Science Press, Dec. 1963.

10. Chan, K. K. and S. K. Rao, "Design of high efficiency circular horn feeds for multibeam reflector applications," *IEEE Transactions on Antennas and Propagation*, Vol. 56, No. 1, 253–258, Jan. 2008.
11. Li, H. and Z. F. Zhong, "Design high power and high efficient multimode feed by MMT," *High Power Laser and Particle Beam*, Vol. 17, No. 8, 1243–1246, 2005.
12. Gentili, G. G., "Properties of TE-TM mode-matching techniques," *IEEE Trans. on Microwave Theory and Technology*, Vol. 39, 1669–1673, Sep. 1991.
13. Gen, M. and R. Cheng, *Genetic Algorithms and Engineering Optimization [M]*, John Wiley & Sons, NY, Jan. 2000.
14. Michael, P. P. and C. Rong, "A high efficiency launcher and mirror system for use in a 110 GHz TE<sub>22,6</sub> mode gyrotron," *Int. J. Infrared Milli. Waves*, Vol. 28, 207–218, 2007.
15. Jamnejad, V. and A. Hoorfar, "Design of corrugated horn antennas by evolutionary optimization techniques," *IEEE Antennas and Wireless Propagation Letters*, Vol. 3, No. 1, 276–279, Dec. 2004.
16. Lucci, L. and R. Nesti, "Phase centre optimization in profiled corrugated circular horns with parallel genetic algorithms," *Progress In Electromagnetics Research*, PIER 46, 127–142, 2008.
17. Potter, P. D., "A new horn antenna with suppressed side lobes and equal beamwidth," *Microwave J.*, Vol. 6, 71–78, Jun. 1963.